Photoinduced reflection spectra of La_2CuO_{4+x} single crystals

A. V. Bazhenov, A. V. Gorbunov, and V. B. Timofeev

Institute of Solid State Physics, Russian Academy of Sciences, Chernogolovka, Moscow Region
(Submitted 15 April 1993)
Zh. Eksp. Teor. Fiz. **104**, 3193–3210 (September 1993)

It is shown that photoinduced optical transitions in La_2CuO_{4+x} single crystals can be detected by a differential light reflection technique. A series of photoinduced electron transitions has been observed in the spectral range 0.1 to 0.6 eV. In a stoichiometric crystal ($x \approx 0$) the intensity of low-energy transitions differs from that of the 0.55-eV transition by a stronger dependence on both the temperature and the power density of exciting light. The properties of these transitions vary with oxygen content. Photoinduced transitions are discussed in the framework of the spin-polaron complex model.

1. INTRODUCTION

Spectroscopy of photoinduced processes is a promising method of investigating electronic and vibrational spectra of dielectric phases of high-T_c superconductors. It allows to study the properties of the spectra versus the density of photoinduced free carriers without introducing defects, which inevitably arise when a crystal is doped. Moreover, pulse technique makes it possible to examine the process dynamics, which is important for understanding the origin of optical excitations in a crystal. The study of the photoinduced absorption (PIA) spectra has shown that a hole created in the valence band of the dielectric phase of a high T_c superconductor either by doping or by optical excitation forms a self-trapped state (STS) in the crystal band gap.[1–3] This gives rise to an absorption band in the mid-infrared range of the spectrum and to local phonon modes. To account for the experimental results the polaron model of STS[2–4] is usually used. However calculations of the PIA in La_2CuO_4 (214) satisfactorily describe only the 0.5 eV band[4] but do not agree with experiment in the range 0.1 to 0.3 eV. In Ref. 4 this was attributed to poor quality of studied samples.

It is most likely that the cause of disagreement between the theory and experiment is of methodological character. The point is that in all previous studies of the PIA in 214 crystals it was the transmission spectrum of a powder in a KBr or CsI matrix that was measured. The size of a 214 grain amounted to $\simeq 1$ μm. Scattering effects important for wavelengths of the order of the grain size were not taken into account. It is just in this spectral range that the largest discrepancies between the polaron theory and experiment take place.

This shortcoming of the PIA method was eliminated by the authors in their study of photoinduced reflection (PIR) in homogeneous dielectric single 214 crystals.[5] It was found that, parallel with the well-known photoinduced electron 0.5 eV transition, there are extra transitions in the range 0.1 to 0.3 eV. The intensities of photoinduced transitions depend on the power density of the exciting laser radiation in a different way. To account for the origin of these electron transitions a model of hole many-particle spin-polaron complexes was suggested.

Low energy electron states near the Fermi surface can play an important role in the mechanism of high T_c superconductivity. To examine the origin of these states and, in particular, applicability of the many-particle spin-polaron complex model we have studied the PIR spectra of semiconducting single La_2CuO_{4+x} crystals versus the oxygen content x, temperature and laser power density. The experimental results are explained qualitatively in the framework of the hole many-particle spin-polaron-complex model.[5]

2. EXPERIMENTAL PROCEDURE

Single 214 crystals were grown by a procedure of dynamic seed growth on a platinum holder[6] with CuO as a solvent. The size of the grown crystals was $4\times4\times4$ mm and their Néel temperature T_N was 250 K. Samples with different T_N were obtained by heat treatment either in vacuum or in oxygen atmosphere. Crystals close to stoichiometric ones ($x=0$, $T_N=318$ K) were prepared by annealing at 600 °C in a 1 Pa vacuum for 4–6 hours. Crystals with large deviation from stoichiometry ($T_N=140$ K) were obtained by annealing in the oxygen atmosphere ($p=1.2\cdot10^5$ Pa) at 600 °C for 3 days. The results of annealing were monitored by the temperature dependence of the magnetic susceptibility. The oxygen content x can be approximately estimated by means of well-known dependences of T_N on the doping impurity content (see, e.g., Ref. 7). In the sudied crystals $T_N=318$, 250, and 140 K and, correspondingly, $x\approx0$, 0.006, and ≈0.01.

To study photoinduced processes in bulk single crystals, it is difficult to use, in practice, the traditional PIA method. Therefore we have used the PIR method.[5] The PIR spectra were measured by a Fourier spectrometer with the incidence of reflected testing light close to normal (the deviation was $\approx10°$). The laser beam exciting the PIR was normal to the sample surface. The reflection spectra were studied in the $\mathbf{E}\perp\mathbf{C}$ polarization ($\mathbf{C}$ is the perpendicular to cuprate planes) with the light wave vector $\mathbf{q}$ parallel to $\mathbf{C}$. The spectral range 35–600 meV was investigated at temperatures from 5 to 200 K. We measured the ratio $R_1(\nu)/R(\nu)$ of the reflection spectra, where $R_1(\nu)$ was the spectrum obtained with continuous irradiation of the crys-

 1063-7761/93/090500-09$10.00

tal by a cw He–Cd or He–Ne laser ($\hbar\omega=2.8$ and 1.96 eV respectively) and $R(\nu)$ was the spectrum without laser excitation. Thus we got the PIR spectrum: $\Delta R/R=[R_1(\nu)-R(\nu)]/R(\nu)$. To increase the signal/noise ratio and decrease the influence of a slow equipment drift on the measurement results we used multiple alternate accumulation of the $R_1(\nu)$ and $R(\nu)$ spectra for 1–2 hours. For this the laser was periodically switched off by a mechanical chopper controlled by the Fourier-spectrometer computer. The reflection spectra were detected either by a DTGS or by a MCT photoresistor cooled by liquid nitrogen. In the latter case scattered laser light affected the receiver performance. Therefore we placed a KRS-5 filter in front of the receiver.

To find the temperature dependence of the spectra the samples were attached to a cold finger in the vacuum chamber of a flowing helium cryostat with the help of a silver paste. The laser excitation power density did not exceed 0.3 W/cm^2 and the corresponding overheat of the samples in our experiment was negligible.

3. ANALYSIS OF PHOTOINDUCED REFLECTION

When nonequilibrium carriers are excited, the variation of the reflection coefficient $R=|(1-\sqrt{\varepsilon})/(1+\sqrt{\varepsilon})|^2$, where $\varepsilon=\varepsilon_1+i\varepsilon_2$, is determined in the general case by variation of both the real (ε_1) and imaginary (ε_2) parts of the dielectric constant. The ratio of the differential dR to the initial dark reflection spectrum R is

$$dR/R=\frac{[(\varepsilon_1-1)(|\varepsilon|+\varepsilon_1)-\varepsilon_2^2]d\varepsilon_1+(2\varepsilon_1+|\varepsilon|-1)\varepsilon_2 d\varepsilon_2}{|\varepsilon|[(\varepsilon_1-1)^2+\varepsilon_2^2][(|\varepsilon|+\varepsilon_1)/2]^{1/2}}$$

$$=A(\nu)d\varepsilon_1+B(\nu)d\varepsilon_2\,. \qquad (1)$$

Here $|\varepsilon|=(\varepsilon_1^2+\varepsilon_2^2)^{1/2}$. We approximate $\varepsilon(\nu)$ by a set of Lorentz oscillators

$$\varepsilon(\nu)=\varepsilon_\infty+\sum \alpha_j N_j/(E_j^2-\nu^2-i\Gamma_j\nu), \qquad (2)$$

where $\alpha_j=4\pi e^2/m_j^*$, E_j is the resonance frequency, Γ_j is the damping, and N_j is the effective density of jth oscillators and is related to the jth oscillator strength S_j by the expression $S_j=\alpha_j E_j^{-2}N_j$. We find that the PIR is proportional to photoinduced changes dN_j of the oscillator density: $dR/R\approx\Sigma C_j(\nu)dN_j$. Besides the photoinduced transition lines, the PIR spectrum can also have narrow false lines at the points where the denominator of (1) vanishes, i.e. when $|\varepsilon|=0$, and also $\varepsilon_1=1$ for $\varepsilon_2=0$.

For the dielectric phase of a high T_c superconductor Eq. (1) becomes much simpler in the mid-infrared range, since $|\varepsilon_1|\gg\varepsilon_2$:

$$dR/R\approx 2d\varepsilon_1/[(\varepsilon_1-1)\varepsilon_1^{1/2}]=A(\nu)d\varepsilon_1 \qquad (3)$$

and the PIR is determined, first and foremost, by the variation of ε_1. In Eq. (3) we have neglected the terms proportional to $(d\varepsilon_1)^2$ and $(d\varepsilon_2)^2$.

Figure 1 shows the reflection spectra $R(\nu)$ and corresponding spectra $\varepsilon_1(\nu)$ and $\varepsilon_2(\nu)$ in a 214 crystal with various oxygen content x. The optical phonon spectrum

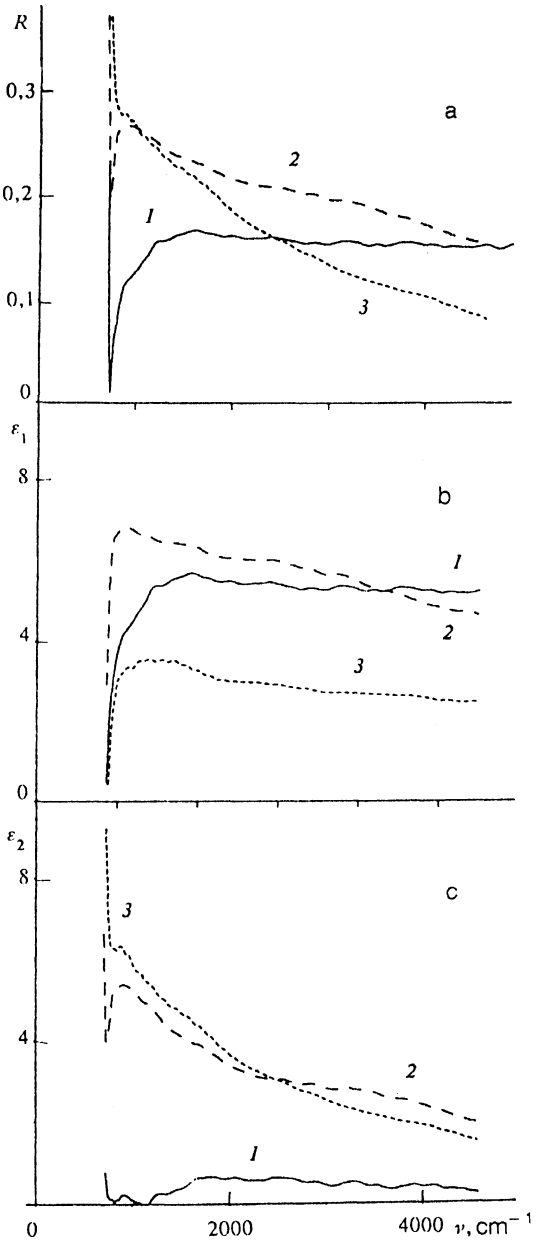

FIG. 1. Reflection spectrum $R(\nu)$ and the real $\varepsilon_1(\nu)$ and imaginary $\varepsilon_2(\nu)$ parts of the dielectric constant of single La_2CuO_{4+x} crystals with different oxygen content: $x\approx 0$, 0.006, and 0.01 for curves *1*, *2*, and *3* respectively (**E**⊥ **C**, $T=5$ K). The curves $\varepsilon_1(\nu)$ and $\varepsilon_2(\nu)$ are calculated with the help of the Kramers-Kronig transformations from the reflection spectra measured in the range 0.005 to 2.7 eV.

visible at $\nu<740$ cm^{-1} is not shown. When the crystal is doped, $\varepsilon_1(\nu)$ varies at first only slightly, and $\varepsilon_2(\nu)$ grows rapidly in the mid-infrared range so that absorption characteristic of cuprate high T_c superconductors is observed. In a 214 crystal we have $\varepsilon_1\simeq\varepsilon_2$ already at $x\simeq 0.005$, and Eq. (1) must be used. The coefficients $A(\nu)$ and $B(\nu)$ are easily found from the spectra of Fig. 1: $A(\nu)$ decreases in a monotonic way and $B(\nu)$ increases with doping (Fig. 2). This can lead to monotonic changes in the PIR amplitude.: the PIR determined by $A(\nu)d\varepsilon_1$ for $x\approx 0$ decreases at first with x and then grows as a result of the growing contribu-

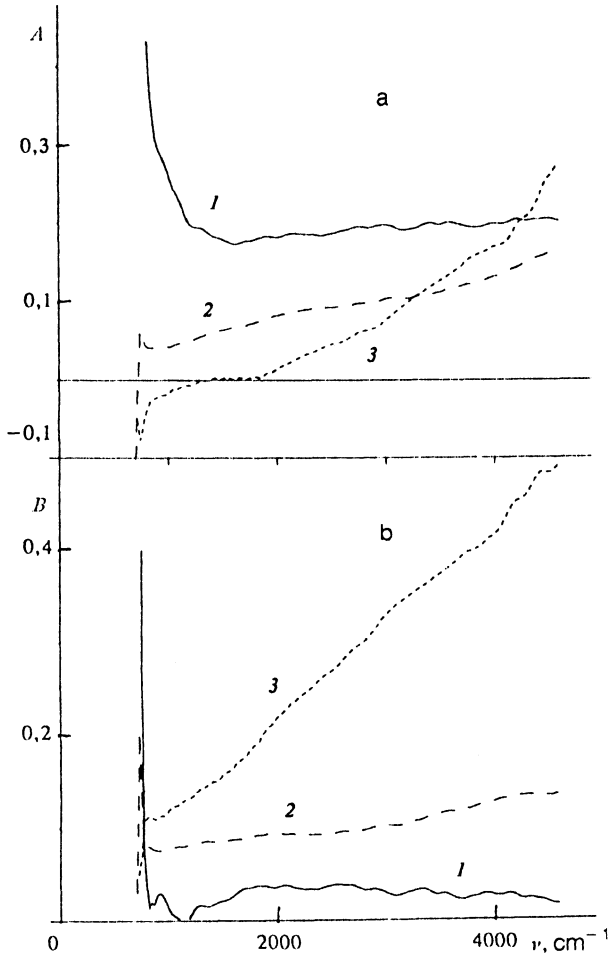

FIG. 2. The coefficients $A(\nu)$ and $B(\nu)$ of Eq. (1) versus the oxygen content x in single La_2CuO_{4+x} crystals: $x\approx 0$, 0.006, and 0.01 for curves *1*, *2*, and *3* respectively. The curves are calculated from the curves $\varepsilon_1(\nu)$ and $\varepsilon_2(\nu)$ of Fig. 1 with the help of Eq. (1) (polarization E⊥ C, $T=5$ K).

tion of the imaginary part of the dielectric constant $B(\nu)d\varepsilon_2$.

For further growth of x the negative contribution of free carriers to $\varepsilon_1(\nu)$ increases. For relatively small x we have $|\varepsilon_1| \ll \varepsilon_2$. Then Eq. (1) takes the form

$$dR/R \approx \sqrt{2}\varepsilon_2^{-5/2}[-(\varepsilon_2+1)d\varepsilon_1+(\varepsilon_2-1)d\varepsilon_2].$$

For a high level of doping the inequality $|\varepsilon_1| \gg \varepsilon_2$ comes into play again, but now, in contrast to the dielectric version (3), we have

$$dR/R \approx \sqrt{2}|\varepsilon_1|^{-3/2}(d\varepsilon_2-\varepsilon_2 d\varepsilon_1).$$

In both cases the PIR diminishes again with growing x, since the effect is proportional to $\varepsilon_2^{-3/2}$ or $|\varepsilon_1|^{-3/2}$.

The reflection-coefficient variation as a result of intensive optical excitation can substantially affect the photoinduced transmission spectrum. It is believed[4] that for dielectric crystals, when $\varepsilon_1 \gg \varepsilon_2$, the relative transmission variation $\Delta T/T$ is connected with the photoinduced high-frequency conductivity $\sigma(\omega)$ by the relation

$$-\Delta T/T=(4\pi s/nc)\sigma(\omega), \qquad (4)$$

where $n=[(\varepsilon_1+|\varepsilon_1|)/2]^{1/2}\approx\varepsilon_1^{1/2}$ is the refractive index, s is the thickness of absorbing medium, and c is the light velocity. Photoinduced variations of the reflection and scattering coefficient are not taken into account.

In the general case, the transmission T, with allowance for single light reflections $R(\nu)$ from two surfaces of a plane-parallel crystal of thickness s, has the form $T=[1-R(\nu)]^2\exp(-\alpha s)$, where $\alpha=2\omega k/c$ is the absorption coefficient and $k=[(|\varepsilon_1|-\varepsilon_1)/2]^{1/2}$. The ratio of the differential dT to the initial dark transmission $T(\nu)$ is

$$-dT/T=\gamma d\varepsilon_1+\delta d\varepsilon_2,$$

$$\gamma=\{(2\varepsilon_1-|\varepsilon_1|-1)/[(n+1)^2+k^2]-s\omega k/c\}/|\varepsilon|,$$

$$\delta=\{(2\varepsilon_1+|\varepsilon_1|-1)k/n[(n+1)^2+k^2]+s\omega n/c\}/|\varepsilon|. \qquad (5)$$

An analysis similar to that for the coefficients $A(\nu)$ and $B(\nu)$ of Eq. (1) shows that in oxygen doped crystals ($x\geqslant 0.005$) a prevailing contribution to the PIA comes from the photoinduced change in ε_2. The PIR effect is small in a broad spectral range, therefore Eq. (4) is valid. In the case of a sufficiently ideal dielectric ($x\approx 0$), when $n^2\approx\varepsilon_1\gg\varepsilon_2$, Eq. (5) acquires the form

$$-dT/T\approx\{(n-1)/[n^2(n+1)]\}d\varepsilon_1+(s\omega/nc)d\varepsilon_2. \qquad (6)$$

The last term in this sum coincides with Eq. (4), since the photo-induced conductivity is $\sigma(\omega)=(\omega/4\pi)d\varepsilon_2$. For $\nu_0=(n-1)/[2\pi n(n+1)s]$ the coefficients in the first and second terms are equal. In the range $\nu\gg\nu_0$ the first term in (6) can be neglected, but for $\nu\simeq\nu_0$ and, especially, for $\nu<\nu_0$ the PIR makes an important contribution to the PIA. In a stoichiometric 214 crystal the refractive index n is ≈ 2 or 3 in the mid-infrared range. Then for $s=0.1$ μm, which is typical of high T_c superconducting films, we have $\nu_0\approx 2700$ cm^{-1}. When a powder of a high-T_c superconductor in the semiconducting phase is studied in a transparent matrix, a typical grain size s is about 1 μm, and the first term in (6) amounts to about 25% of the second at $\nu\leqslant 1100$ cm^{-1}. In fact, owing to light scattering, the relative role of reflection in the transmission spectrum of powderlike samples is even more important, therefore the PIR contribution can be large even at higher frequencies.

The photoinduced reflection has some advantages in comparison with the PIA used in powderlike sample studies. The PIR method can be used to investigate the properties of bulk single crystals. Light scattering effects are thereby excluded and a possibility of studying the anisotropy of photoinduced optical transitions arises. It is also important that in the case of stoichiometric (dielectric) crystals PIR measurements in the mid-infrared give information about changes in the dielectric function, namely in the real part of the dielectric constant.

4. EXPERIMENTAL RESULTS AND DISCUSSION

The reflection spectrum of a dielectric 214 crystal ($T_N=318$ K) receives no contribution from free carriers in the E⊥ C geometry in the range 0.005–0.6 eV. Moreover, in the range 0.15–0.5 eV there is practically no ab-

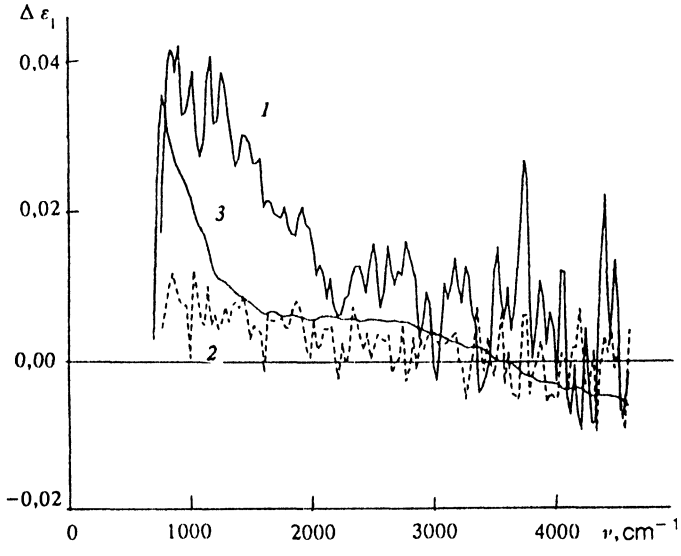

FIG. 3. The spectra of photoinduced variation of the real part $\varepsilon_1(\nu)$ of the dielectric constant in a single La_2CuO_4 crystal with $T_N=318$ K ($x\approx 0$) for nonequilibrium carrier excitation by a continuous He–Cd ($\hbar\omega=2.8$ eV, curve *1*) and a He–Ne laser ($\hbar\omega=1.96$ eV, curve *2*). The temperature is 5 K, and the density of laser excitation power is 0.2 W/cm^2. Curve *3* is the difference between the $\varepsilon_1(\nu)$ spectra of an oxygen doped La_2CuO_{4+x} ($T_N=250$ K, $x\approx 0.006$) and a stoichiometric crystal ($T_N=318$ K, $x\approx 0$). Polarization $E\perp C$, $T=5$ K.

sorption typical of oxygen doped Sr compounds, and $\varepsilon_1(\nu)\approx\varepsilon_\infty\approx 5.3$, as seen from Fig. 1. Both factors are indicative of a high degree of stoichiometry of the given crystal whose oxygen content x is about zero. In this case Eq. (3) is valid, since $\varepsilon_1\gg\varepsilon_2$ (see Fig. 1), and the PIR is determined by changes in the real part of the dielectric constant, $\Delta\varepsilon_1(\nu)$.

In Fig. 3 curve *1* shows $\varepsilon_1(\nu)$ in this crystal in the $E\perp C$ polarization, when nonequilibrium carriers are excited by a He–Cd laser ($\hbar\omega=2.8$ eV). The spectrum is obtained by dividing the measured PIR by the coefficient $A(\nu)$ (Fig. 2). It is worth noting that the spectral dependence of PIR in our case radically differed from that when the crystal is overheated by laser radiation. For an insufficient thermal contact of the sample the spectral intensity grew in a monotonic way with the wave number ν. The reproducibility of the absolute value of the spectrum was very low. When the frequency of exciting light (an He–Ne laser, $\hbar\omega=1.96$ eV) decreases, the PIR intensity falls off dramatically (curve *2*). The studies of absorption[8] and photoconductivity[9] spectra have shown that the fundamental absorption edge determined by interband transitions with charge transfer coincides with the energy $\hbar\omega\approx 2.1$ eV in 214 crystals. Thus, hole and electron generation just in the valence and conduction bands gives rise to photoinduced 0.1–0.5 eV transitions. If photoexcitation is in the dielectric gap region, the PIR is absent.

As already noted in a series of studies where the PIA was investigated in powdered semiconducting phases of high T_c superconductors, in a single 214 crystal the photoinduced transitions are similar to those arising for doping with acceptor impurities. In our case curve *3* in Fig. 3 shows the change in $\varepsilon_1(\nu)$ when oxygen is introduced into the crystal: $\Delta\varepsilon_1=\varepsilon_1^1-\varepsilon_1^0$, where $\varepsilon_1^1(\nu)$ and $\varepsilon_1^0(\nu)$ are the spectra of crystals with $T_N=250$ and 318 K respectively. Similarity of spectra *1* and *3* indicates that the nonequilibrium carrier excitation really leads to an effect similar to crystal doping with impurities. Thus, the origin of spectral changes in both cases is the same.

Important information about photoinduced transitions is provided by their intensity as a function of the density of interband-excitation power I. In Ref. 1 the PIA spectrum of the 214 powder was interpreted as two transitions with energies 0.16 and 0.62 eV. It was shown that both their intensities depend on I as I^α; in particular, at $T=4.2$ K we have $\alpha=0.25$. A similar result was obtained by us for the PIR spectra of oxygen doped crystals in the range $I\leqslant 0.3$ Wt/cm^2. This is shown in Fig. 4b, where the spectra of a single 214 crystal with $T_N=140$ K ($x\approx 0.01$) are shown. The same was observed also in the stoichiometric 214 crystal ($T_N=318$ K) for $I\leqslant 50$ mWt/cm^2. However, at higher power densities the stoichiometric 214 crystal exhibited a superlinear dependence of the low energy PIR intensity (I_L) with respect to the 0.55 eV transition (I_H), i.e. $I_L(I)\simeq I_H(I)^\beta$ where $\beta>1$ (Fig. 4a).

With increasing temperature the low-energy PIR intensity decreases much more rapidly than for the 0.55 eV transition in the crystal with $x\approx 0$ (Fig. 5). The PIR in the mid-infrared is observed only at $T<150$ K, whereas similar transitions in doped crystals are clearly seen even at $T>300$ K.

Figure 6 shows the dependence of the PIR spectrum ($E\perp C$) on the oxygen content in a single 214 crystal at $T=5$ K. The PIR intensity is the greatest in the stoichiometric crystal, falls off for $x\approx 0.006$, and grows again for $x\approx 0.01$. We have called attention in Sec. 3 to a possible nonmonotonic dependence of the PIR on crystal doping, and related it to a crossover from the predominant contribution of the photoinduced change $\Delta\varepsilon_1$ to the growing effect of $\Delta\varepsilon_2$. As the PIR spectrum analysis in the Lorentz oscillator approximation has shown, the density dN_j of photoinduced oscillators varies monotonically.

If we try to approximate the PIR by two electronic transitions (oscillators), ν_L and ν_H, of low and high energy respectively, we must assume an extraordinarily large increase in the damping Γ_L for the transition ν_L when the temperature increases from 5 to 50 K, namely $\Gamma_L\approx 0.25$ and 0.5 eV, which is absolutely unfounded. If we assume that the electron oscillator damping has a relatively weak temperature dependence, the best approximation is achieved when the spectrum is described by four Lorentz oscillators. Additional studies of the temperature dependence of the infrared reflection spectra of 214 single crystals doped by oxygen showed that in the mid-infrared the spectrum is approximated by four Lorentz oscillators.[10] Therefore Fig. 7a shows the approximation of the photoinduced variation $\Delta\varepsilon_1$ in a stoichiometric crystal by oscillators with resonance frequencies $E_j=550$, 240, 156, and 110 meV. Expansion in the contribution of separate oscillators (Fig. 7b), yields substantially different partial weights: $dN_j=3\cdot 10^{18}$, $3\cdot 10^{17}$, $8\cdot 10^{16}$ and 10^{16} cm^{-3} re-

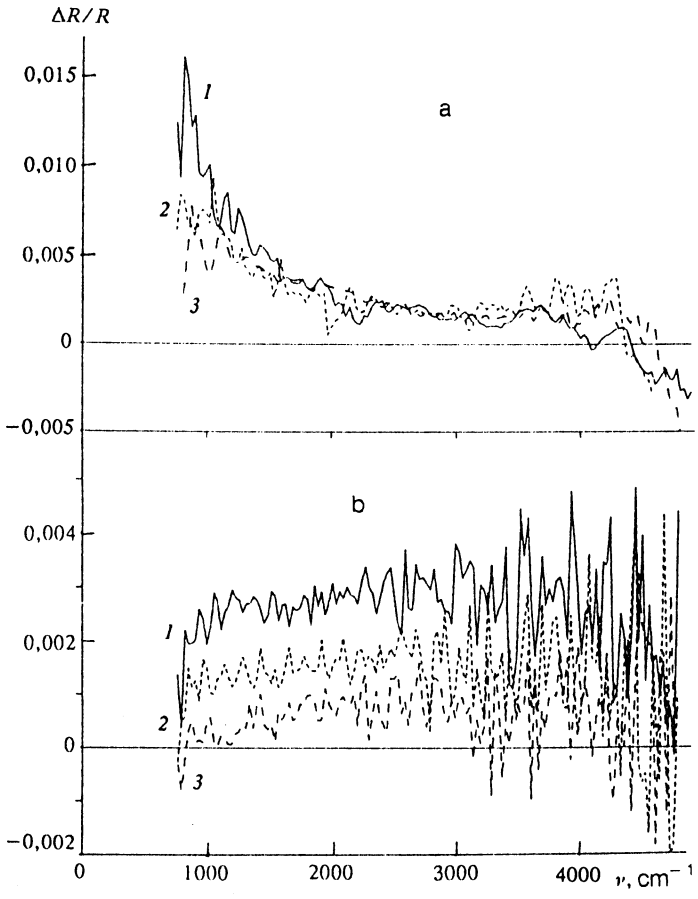

FIG. 4. The photoinduced reflection spectrum versus the density of He–Cd laser power in single La_2CuO_{4+x} crystals: (a) $T_N=318$ K ($x\approx 0$) and (b) $T_N=140$ K ($x\approx 0.01$). The highest density of laser radiation power is 0.2 W/cm^2. The curves *1–3* in Fig. 4(a) correspond to power densities I, $I/2$, and $I/4$, and the curves in Fig. 4(b) to I, $I/10$ and $I/40$. The spectra are smoothed off.

spectively, and dampings $\Gamma_j\approx 550$, 220, 90, and 30 meV at $T=5$ K and at an excitation power density $I=0.2$ Wt/cm^2. In Eq. (2) the effective mass m^* was taken equal to the free electron mass. A PIR analysis in the framework of the suggested approximation has shown a monotonic dependence of the densities of photoinduced oscillators on the oxygen content in the crystal (Fig. 8).

Thus, we have found that interband excitation of single 214 crystals in the spectral range 0.1–0.6 eV produces several photoinduced electron transitions. They are similar to transitions arising when a crystal is doped by acceptor impurities and have the following features:

1) in a stoichiometric 214 crystal the intensity of low-energy transitions with respect to the transition $E_1=0.55$ eV has a superlinear dependence on the power density I at a high level of interband excitation;

2) in oxygen-doped crystals the intensities of photoinduced 0.1–0.6 eV transitions have the same I-dependence;

3) the intensity of low-energy transitions decreases much more rapidly with increasing temperature than that of the E_1 transition in the stoichiometric 214 crystal. The PIR is observed only at $T<150$ K.

We believe that an electron injected into the conduction band by light is trapped there. A hole created in the

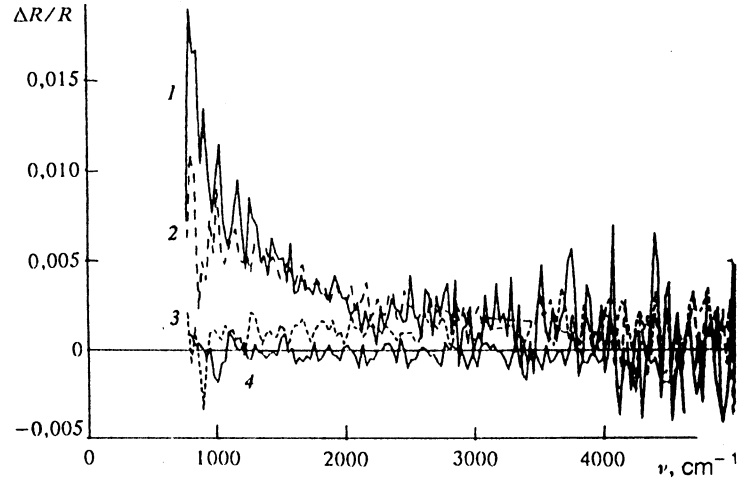

FIG. 5. The temperature dependence of the PIR spectrum in a stoichiometric single La_2CuO_4 crystal ($T_N=318$ K): spectra *1–4* correspond to $T=5$, 50, 100, and 150 K respectively. The power density of laser radiation is 0.2 W/cm^2, polarization E⊥ C. The spectra are smoothed off.

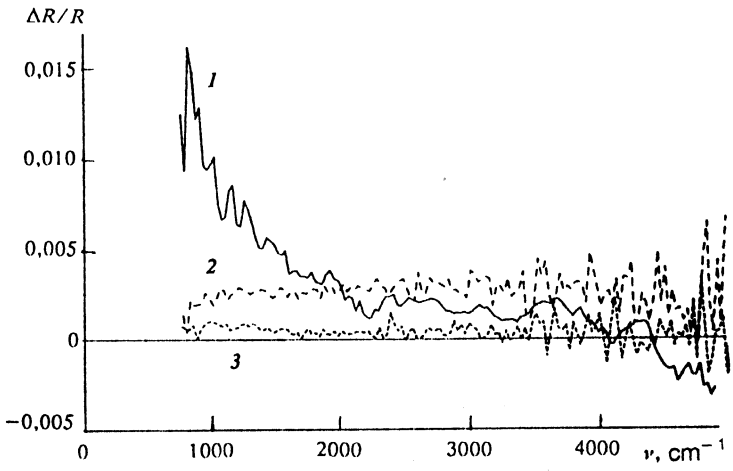

FIG. 6. The effect of the oxygen content on the photoinduced reflection spectrum in a single La_2CuO_{4+x} crystal: $x \approx 0$, 0.006, and 0.01 for the spectra *1*, *2*, and *3* respectively. Polarization $E \perp C$, $T = 5$ K, and the power density of the He–Cd laser is 0.2 W/cm^2.

valence band as a result of optical excitation or doping is trapped and forms in the crystal band gap a self-trapped state (STS) associated with the optical transition $E_1 = 0.55$ eV with the half-width $\Gamma_1 \approx E_1$. Doping 214 crystals with oxygen leads to p-type conductivity. Therefore the fact that the photoinduced spectra are identical with the doped crystal spectrum indicates that the studied optical transitions are determined exactly by hole STS. The photoinduced transitions vanish at $T \geqslant 150$ K, whereas in doped crystals similar transitions are observed at $T > 300$ K. The difference is connected with the intensities of photoinduced transitions being determined by recombination of optically injected electrons and holes. At $T \geqslant 150$ K practically all photoelectrons are thermally activated from traps into the conduction band, where they recombine with holes and the PIR vanishes.

The superlinear increase in the low-energy transition intensity with respect to E_1 in a stoichiometric crystal with increasing interband excitation intensity I and, correspondingly, photohole density $p (p \simeq I^{\alpha})$ indicates that the low-energy transitions correspond most likely to many-particle complexes of a hole STS. For the E_1 transition the photoinduced oscillator density dN_1 is proportional to p, $dN_1 \simeq p$. At the same time the process of formation of many-particle complexes E_j as a result of 2-, 3-, and 4-particle hole collisions obeys the law $dN_2 \simeq p^2 + pN_1$,

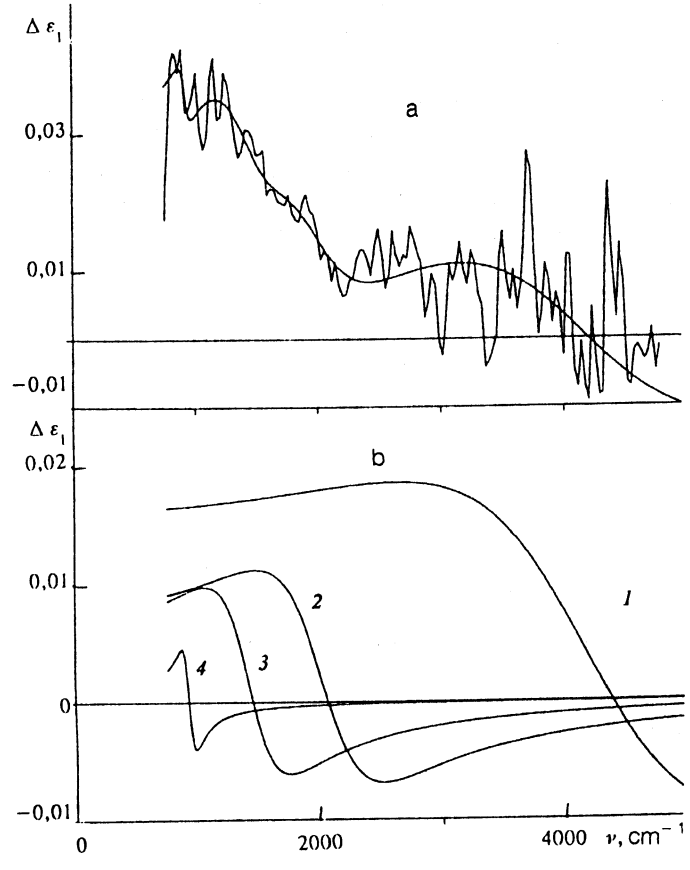

FIG. 7. (a) The approximation of the photoinduced $\Delta\varepsilon_1$ spectrum at $T = 5$ K by four Lorentz oscillators in accordance with Eqs. (2) and (3). The curve $\Delta\varepsilon_1$ is found by dividing the photoinduced reflection spectrum 1 in Fig. 6 by the function $A(\nu)$ (curve *1* in Fig. 2a); (b) Expansion of this spectrum in contributions of separate oscillators *1–4* with resonance frequencies $E_j = 550$, 240, 156, and 110 meV respectively.

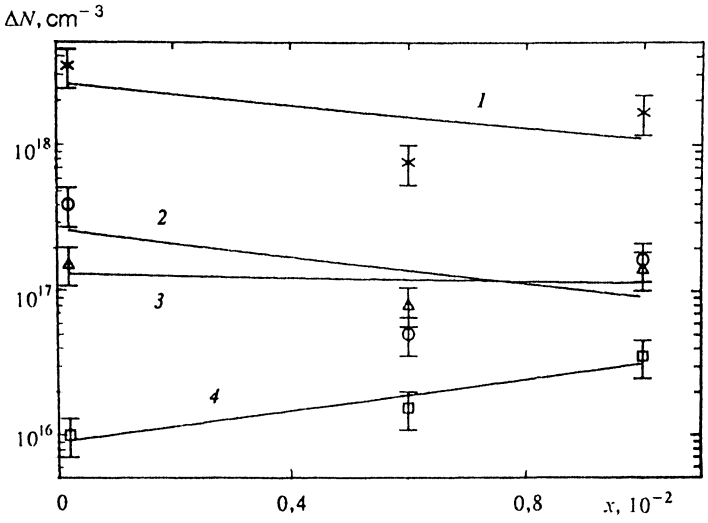

FIG. 8. The densities dN_j of photoinduced oscillators with resonance frequencies E_j=110, 156, 240, and 550 meV (curves *1–4* respectively) versus the oxygen content x in single La_2CuO_{4+x} crystals. Temperature is 5 K, and the density of interband excitation power is 0.2 W/cm^2.

$dN_3 \simeq p^3 + p^2 N_1 + p N_2$ etc., where N_j is the dark concentration of STS with j holes. In a stoichiometric crystal we have $N_j \approx 0$, therefore $dN_j \approx p^j$, i.e. the intensity of transitions corresponding to many-particle complexes depends superlinearly on p in contrast with the E_1 transition. In oxygen doped crystals $p \ll N_j$ and photoinduced complexes are formed mainly by hole attachment to already existing complexes, $dN_j \simeq p N_{j-1}$. Therefore the intensities of all transitions have the same I-dependence. A similar dependence in the crystal with T_N=318 K for a low excitation level is explained by a small initial STS density, as seen from the spectra of Fig. 1 ($\varepsilon_2 \approx 0.1$ for $\hbar\omega \approx 0.11$ eV), and connected with a small deviation from stoichiometry.

The many-particle-complex model makes it possible to explain also the temperature dependence of the photoinduced transition intensity. When electrons are thermally activated from their traps to the conduction band, p decreases. Therefore a more drastic temperature dependence of the low-energy transition intensities in a stoichiometric 214 crystal seems natural, since in this case $dN_j \approx p^j$.

The densities dN_1 and dN_2 of photoinduced oscillators (E_j=0.55 and 0.24 eV) decrease with increasing oxygen content (Fig. 8). This can be explained by the decreasing lifetime of nonequilibrium carriers and, consequently, of their densities as a result of introducing an excess x of oxygen into the crystal. However, dN_3 (E_3=0.156 eV) practically does not change, and dN_4 (E_4=0.11 eV) grows noticeably with x. This can be accounted for by the fact that for $x \geqslant 0.005$ the STS complexes are formed mainly by attachment of a hole to existing complexes, $dN_j \simeq p N_{j-1}$. The infrared reflection spectra in Fig. 1 show that with increasing x the intensities of E_j transitions increase monotonically, the intensities of low-energy transitions increasing more than the others. Therefore the decrease in dN_j caused by decreasing p can be compensated for by the increasing the initial complex density N_{j-1} and can increase the density of low-energy photoinduced oscillators with increase of x.

Thus, the suggested model of many-particle hole STS makes it possible to explain qualitativly the presence of a series of electron transitions in the mid-infrared in semiconducting phases of high T_c superconductors, and their properties versus temperature, oxygen content, and density of the power exciting the nonequilibrium carriers in crystals. An elucidation of the origin of the STS and its many-particle complexes is therefore urgent. At present the polaron model is being discussed in the literature, in view of the presence of local phonon modes in PIA spectra,[3] attributed to crystal lattice relaxation near the hole as a result of its Coulomb interaction with crystal ions. However polaron absorption calculations account for the 0.55 eV line but do not explain the 0.1–0.3 eV[4] transitions with properties of many-particle complexes.

The polaron complex formation is inhibited by the Coulomb repulsion. Without excluding the possibility of the polaron effect, we call attention to the results of magnetic studies of the semiconducting phase of high T_c superconductors. Theoretical calculations show that the interaction of hole spins with copper can also lead to the formation of the STS of the ferron[11–13] (spin-polaron,[14] magnetic polaron[15]) type, which is a ferromagnetic cluster 30–40 Å in diameter.[12,13] Late calculations[16] indicate that the STS can exist as an afmon, i.e. "a carrier+a microregion of another antiferromagnetic phase," or as a drop of spin liquid. The exchange interaction provides mutual STS attraction to form complexes.[14,16] The available experimental data do not make it possible to specify the structure of such an STS. In what follows we will use, for definiteness, the term "spin-polaron" (ferron), implying the feasibility of afmon, spin-liquid, and other structures. In fact, the suggested model of many-particle hole STS can be regarded as further development of well-known theoretical[17,18] and experimental[7,19,20] studies. In Refs. 17 and 18 it was shown that free holes in a two-dimensional antiferromagnet are unstable to decay into a dielectric antiferromagnetic phase and into a phase enriched by holes. A similar conclusion follows from the results of neutron-diffraction studies of an oxygen-rich 214 structure,[7,19] as well as of photoconductivity in $YBa_2Cu_3O_{7-x}$ single crystals and epitaxial $DyBa_2Cu_3O_{7-x}$ films.[20] The model of

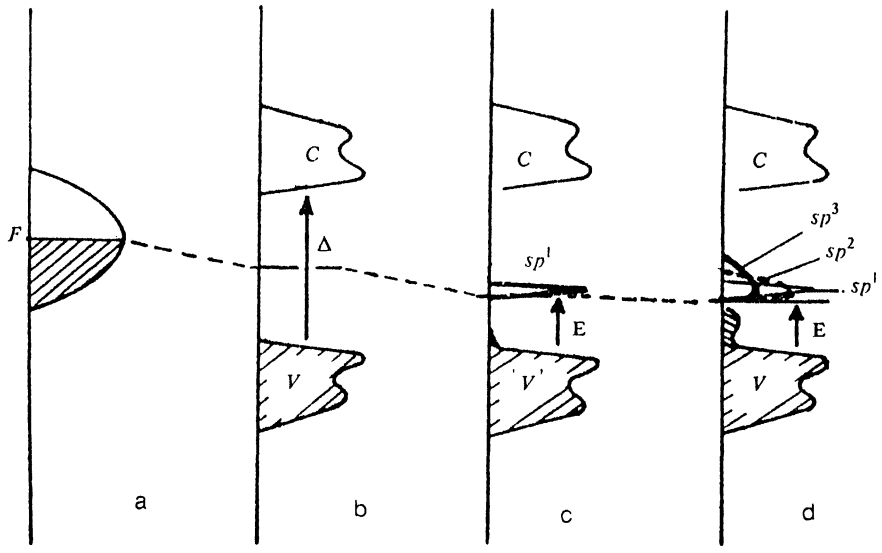

FIG. 9. The diagram of semiconducting phase energy structure in La_2CuO_{4+x}: (a) one-electron approximation; (b) strong-coupling approximation; (c) formation of spin-polaron states upon introducing holes into the crystal ($x>0$); and (d) formation of spin-polaron complexes for further increase in hole density in the crystal.

spin-polarons and their many-particle complexes is attractive in that it fits in with modern notions of the mechanism of destruction of a three-dimensional antiferromagnetic ordering in the semiconducting phase of high T_c superconductors. It is believed that a strong dependence of the Néel temperature T_N on the hole density in cuprate high-T_c superconductors is accounted for by the competition of anti- and ferromagnetism (see, e.g., Refs. 12, 13, and 21 and citations therein).

It is worth paying attention to calculations carried out in the framework of the generalized tight-binding scheme.[22,23] In ordinary semiconductors impurity levels are due to crystal-potential distortions in the vicinity of the defect. These studies have shown that when holes are introduced into a dielectric with strong electron correlations, states may arise in the crystal band gap without crystal-potential distortion by the defect. Thus, the band structure of the dielectric phase of a high T_c superconductor can be imagined as follows. In the one-electron approach, for example, a 214 crystal must be a metal with a half-filled band originating from hybridization of the $Cu3d_{x^2-y^2}$ and $O2p_{x,y}$ states (Fig. 9a). The semiconducting gap $\Delta=2.1$ eV (Fig. 9b) is due to strong electron correlations. Introduction of a hole into the valence V-band (by doping or photoinjection) creates a new state in the band gap as a result of spin interaction of the hole and copper.[22,23] This state can possibly be the hole STS state of the spin-polaron type[15–20] discussed above (sp^1 in Fig. 9c). Crystal-lattice relaxation is likely to contribute to the STS energy as well. According to Ref. 23, along with a narrow hole state in the band gap, a tail of the density of states is formed near the top of the V-band by spin and charge fluctuations. It is expected that the maximum of its density shifts to the Fermi level with increasing hole density.

We assume that the wide optical transition $E_1=0.55$ eV (the half-width $\Gamma\simeq 0.5$ eV) corresponds to destruction of this STS state by optical excitation of a self-trapped hole into the V-band. In such a case, its position E above the top of the V-band is determined by the red edge of the transition E_1, i.e. $E\simeq 0.1$ eV [see the expansion of $\varepsilon_2(\nu)$ in Fig. 2 of Ref. 5]. The energy positions of spin-polaron complexes (sp^1, sp^2, and sp^3 in Fig. 9d) differ only slightly from the positions of single spin-polarons. This is evidenced, first, by the close values of red edges of the corresponding optical absorption lines, $E\simeq 0.1$ eV, and second, by dc conductivity measurements in the studied crystals. We have found that in the stoichiometric 214 crystal in the temperature range $T=5$–300 K the conductivity is governed by the Mott law. In oxygen-doped crystals the Mott mechanism of hopping conductivity gives way to nearest-neighbor hops at $T=15$–30 K. The activation energy is low, about 5 meV. Therefore the spin-polaron states through which, in our opinion, the conductivity at low temperatures in a semiconducting 214 crystal is realized differ only slightly in energy. This is supported by the fact that the Coulomb repulsion of holes in the complex can be compensated for by gain in spin system energy, since complex formation entails a decrease in the number of broken spin configurations.[14] The important difference between the spectral positions of the maxima of optical absorption lines connected with STS complexes ($E_i=0.11$–0.55 eV) can be accounted for by the fact that the localization size of the self-trapped hole wave function increases and, therefore, the uncertainty in momentum decreases on going from a single STS to its many-particle complexes. Correspondingly, the energy range of the V-band states taking part in optical transitions becomes more narrow.

In such a model the Fermi level (F) is pinned[23] by STS complexes and does not practically change position under crystal doping. This agrees with the results of photoemission research,[24–26] where it has been shown that the Fermi level position, with respect to the V-band basic features, does not change on going from the semiconducting to superconducting phase of cuprate high T_c superconductors. Thus, we reject the traditional semiconductor rigid-band model.

5. CONCLUSION

In the present study the photoinduced transitions in single crystals of cuprate oxides have been investigated for

the first time, using the semiconducting phase of La_2CuO_{4+x} (214) with different oxygen content x. We have developed a procedure of photoinduced light reflection (PIR). In contrast to the previously used method of photoinduced absorption (or, more exactly, transmission) by inhomogeneous powderlike samples, the suggested procedure makes it possible to investigate bulk ideal single crystals and exclude the effect of photoinduced light scattering on the measurements.

It has been shown that interband excitation of single 214 crystals in the range 0.1–0.6 eV gives rise to several electron transitions active in $\mathbf{E}\perp\mathbf{C}$ polarization. They are similar to transitions arising when crystals are doped with acceptors and have the following properties: (1) in a stoichiometric 214 crystal the low-energy transition intensity, with respect to the transition $E_1=0.55$ eV, has a superlinear power density dependence for a high level of interband excitation; (2) in oxygen doped crystals the intensities of photoinduced 0.1–0.6 eV transitions have the same I-dependence; (3) the intensity of low-energy transitions decreases much more rapidly with increasing temperature than that of the E_1 transition in stoichiometric 214 crystals.

To account for the origin and properties of photoinduced transitions we have suggested a model based upon formation of hole self-trapped states, due to spin interaction of a nonequilibrium hole and copper atoms, and their many-particle complexes. Evidently, they include crystal lattice relaxation as well. To find the specific structure of such a state [spin-polaron (ferron), afmon, spin liquid...] we need further investigations.

This work has been supported partly by the American Physical Society through a Soros Foundation Grant and carried out in the framework of the "Spectrum" project, N 90237, of the State High T_c Superconductivity Program. The authors are grateful to M. Yu. Maksimuk for his help with the data processing and to A. A. Zakharov for supplying the single crystals.

[1] Y. H. Kim, S. W. Cheong, and Z. Fisk, Phys. Rev. Lett. **67**, 2227 (1991).
[2] H. J. Ye, R. P. McCall, W. E. Farneth, E. M. McCarron, and A. J. Epstein, Phys. Rev. B **44**, 237 (1991).
[3] D. Mihailovic, C. M. Foster, K. F. Voss, T. Mertelj, and I. Poberaj, Phys. Rev. B **44**, 237 (1991).
[4] D. Mihailovic, C. M. Foster, K. F. Voss, and A. J. Heeger, Phys. Rev. B **42**, 7989 (1990).
[5] A. V. Bazhenov, A. V. Gorbunov, and V. B. Timofeev, Pis'ma Zh. Eksp. Teor. Fiz. **56**, 604 (1992) [JETP Lett. **56**, 587 (1992)].
[6] S. N. Barilo, A. P. Gel', S. A. Guretskiĭ *et al.*, Sverkhprovod. Fiz. Khim. Tekh. **2**, 138 (1989) [Supercond. Phys. Chem. Tech.].
[7] B. Dabrowski, J. D. Jorgensen, D. G. Hinks *et al.*, Physica C **162–164**, 99 (1989).
[8] N. V. Abrosimov, A. V. Bazhenov, A. V. Gorbunov *et al.*, Supercond. Fiz. Khim. Tekh. **4**, 2165 (1991) [Supercond. Phys. Chem. Tech.].
[9] T. Thio, R. G. Birgeneau, A. Cassanho, and M. A. Kasyner, Phys. Rev. B **42**, 10800 (1990).
[10] A. V. Bazhenov, A. V. Gorbunov, K. B. Rezchikov *et al.*, Physica C **208**, 197 (1993).
[11] E. L. Nagaev, Usp. Fiz. Nauk **117**, 437 (1975) [Sov. Phys. Usp. **18**, 863 (1976)].
[12] V. Hizhnyakov and E. Sigmund, Physica C **156**, 655 (1988).
[13] V. Hizhnyakov, N. Kristoffel, and E. Sigmund, Physica C **160**, 119 (1989).
[14] R. F. Wood and J. F. Cooke, Phys. Rev. B **45**, 5585 (1992).
[15] N. F. Mott, *Metal-Insulator Transitions* (Taylor & Francis, London, New York, Philadelphia, 1990), p. 222.
[16] E. L. Nagaev, Zh. Eksp. Teor. Fiz. **103**, 252 (1993) [JETP **76**, 138 (1993)].
[17] L. P. Gor'kov and A. V. Sokol, Pis'ma Zh. Eksp. Teor. Phys. **46**, 333 (1987) [JETP Lett. **46**, 420 (1987)].
[18] V. J. Emery, S. A. Kivelson, and H. Q. Lin, Phys. Rev. Lett. **64**, 475 (1990).
[19] J. D. Jorgensen, B. Dabrowski, S. Pei *et al.*, Phys. Rev. B **38**, 11337 (1988).
[20] G. Yu, C. H. Lee, A. J. Heeger *et al.* Phys. Rev. B **45**, 4964 (1992).
[21] Yu. A. Izyumov, H. M. Plakida, and Yu. N. Skryabin, Usp. Fiz. Nauk **159**, 621 (1989) [Sov. Phys. Usp. **32**, 1060 (1989)].
[22] S. G. Ovchinnikov, Zh. Eksp. Teor. Fiz. **102**, 534 (1992) [JETP **75**, 283 (1992)].
[23] H. Matsumoto, M. Sasaki, and M. Tachiki, Phys. Rev. B **43**, 10264 (1991).
[24] N. Nukker, J. Fink, J. C. Fuggel *et al.*, Phys. Rev. B **37**, 5158 (1988).
[25] N. Takahashi, H. Matsuyama, H. Katayama-Yoshida *et al.*, Phys. Rev. B **39**, 6636 (1989).
[26] A. J. Arko, R. S. List, R. J. Barlett *et al.*, Phys. Rev. B **40**, 2268 (1989).

Translated by E. Khmelnitski